THE JOURNAL OF BIOLOGICAL CHEMISTRY
Vol. 276, No. 22, Issue of June 1, pp. 19483–19490, 2001
Printed in U.S.A.

The Dynamics of the Relay Loop Tryptophan Residue in the *Dictyostelium* Myosin Motor Domain and the Origin of Spectroscopic Signals*

Received for publication, December 4, 2000, and in revised form, February 16, 2001
Published, JBC Papers in Press, February 22, 2001, DOI 10.1074/jbc.M010886200

András Málnási-Csizmadia‡, Mihály Kovács‡§¶, Robert J. Woolley‡, Stanley W. Botchway‖, and Clive R. Bagshaw‡

From the ‡Department of Biochemistry, University of Leicester, Leicester LE1 7RH and ‖The Central Laser Facility, Rutherford Appleton Laboratory, Chilton, Didcot, OX11 0QX, United Kingdom, and the §Department of Biochemistry, Eötvös University, Budapest H-1088, Hungary

Steady-state and time-resolved fluorescence measurements were performed on a *Dictyostelium discoideum* myosin II motor domain construct retaining a single tryptophan residue at position 501, located on the relay loop. Other tryptophan residues were mutated to phenylalanine. The Trp-501 residue showed a large enhancement in fluorescence in the presence of ATP and a small quench in the presence of ADP as a result of perturbing both the ground and excited state processes. Fluorescence lifetime and quantum yield measurements indicated that at least three microstates of Trp-501 were present in all nucleotide states examined, and these could not be assigned to a particular gross conformation of the motor domain. Enhancement in emission intensity was associated with a reduction of the contribution from a statically quenched component and an increase in a component with a 5-ns lifetime, with little change in the contribution from a 1-ns lifetime component. Anisotropy measurements indicated that the Trp-501 side chain was relatively immobile in all nucleotide states, and the fluorescence was effectively depolarized by rotation of the whole motor domain with a correlation time on 50–70 ns. Overall these data suggest that the backbone of the relay loop remains structured throughout the myosin ATPase cycle but that the Trp-501 side chain experiences a different weighting in local environments provided by surrounding residues as the adjacent converter domain rolls around the relay loop.

Spectroscopic signals from tryptophan residues have long been used as an empirical tool for distinguishing different nucleotide states of the myosin ATPase cycle (1–3). Interest in this topic has been rekindled by the elucidation of crystal structures of the myosin motor domain in which the location and environments of the tryptophan residues can be compared in several different states (4–8). Recently, site-directed mutagenesis has been used to define the contributions of individual tryptophan residues to the observed spectroscopic signals (9–12). These studies were preceded by and have been supplemented with chemical approaches to isolate the spectroscopy-sensitive residues (13–15). There is now unanimous agreement that the conserved tryptophan residue located on the relay loop of the lower 50 kDa domain (skeletal myosin Trp-510, smooth myosin Trp-512, and *Dictyostelium* Trp-501) is uniquely associated with the fluorescence enhancement observed during ATP hydrolysis. The hydrolysis step itself appears coupled to the open → closed transition, identified crystallographically (16). It appears that the open → closed transition is actually responsible for the structural changes in the vicinity of the spectroscopy-sensitive tryptophan residue, but the hydrolysis reaction serves to pull the equilibrium toward the predominant steady-state intermediate in the *Dictyostelium discoideum* motor domain, M*·ADP·P_i or the equivalent M**·ADP·P_i intermediate in vertebrate skeletal myosins (12). The origin of the smaller fluorescence enhancement seen on nucleotide binding to skeletal and smooth myosin is less clear and is species-specific. In smooth muscle myosin the enhancement induced by ADP binding appears to emanate from Trp-512 (10), whereas the equivalent residue in *D. discoideum*, Trp-501, responds with a fluorescence quench (12). The fluorescence enhancement associated with ADP binding to skeletal myosin may have its origins in the nonconserved Trp-131 residue (15). In this work we address further properties of the relay loop tryptophan of *D. discoideum* myosin motor domain, Trp-501.

The kinetic mechanism of ATP hydrolysis by all myosins II appears similar. Although the absolute values of the rate constants of equivalent steps may differ among species, their ratios are such that a similar distribution of nucleotide states is obtained during the steady state. In the case of the *D. discoideum* motor domain the mechanism may be summarized as in Reaction 1

$$M+ATP \leftrightarrow (M\cdot ATP) \rightarrow M\dagger\cdot ATP \leftrightarrow (M^*\cdot ATP) \leftrightarrow M^*\cdot ADP\cdot Pi \leftrightarrow$$
$$(M\dagger\cdot ADP\cdot Pi) \leftrightarrow M\dagger\cdot ADP+Pi \leftrightarrow (M\cdot ADP) \leftrightarrow M+ADP$$

REACTION 1

where † represents a quenched state, and * is an enhanced state of Trp-501 (12). States in parentheses are present at near negligible concentrations under most conditions, but their existence is implied by kinetic arguments. Under the usual conditions of assay, the M*·ADP·P_i state predominates during the steady-state hydrolysis of ATP (which is equivalent to the M**·ADP·P_i state of vertebrate myosins in which other tryptophan residues may contribute to the overall fluorescence enhancement (17, 18)). By adding the P_i analog AlF_4^- to the *D. discoideum* M†·ADP complex, a stable M*·ADP·AlF_4 complex can be made which has an enhanced fluorescent state and provides a useful analog of the M*·ADP·P_i state for spectroscopic

* This work was supported in part by the Biotechnology and Biological Sciences Research Council and the Wellcome Trust. The costs of publication of this article were defrayed in part by the payment of page charges. This article must therefore be hereby marked "*advertisement*" in accordance with 18 U.S.C. Section 1734 solely to indicate this fact.
¶ Visit funded by a Hungarian State Eötvös fellowship.
** To whom correspondence should be addressed. E-mail: crb5@le.ac.uk.

studies (12). Care is required, however, in relating a particular analog state to particular ATPase intermediate because in many cases these complexes exist as a mixture of conformations.

Fluorescence quenching studies with acrylamide and iodide indicate that on binding nucleotide, Trp-501 (or equivalent) becomes slightly less accessible to solvent and is protected further after hydrolysis to give the long lived M*·ADP·P_i species (10, 12, 15). The crystal structures are generally in accord with the spectroscopic results in that, when resolved, Trp-501 (or equivalent) points toward the converter domain, but it is not internalized completely and has limited exposure to solvent (5, 6). Interestingly, in the case of the *Dictyostelium* crystal structures, the main chain bearing Trp-501 is usually unresolved in nucleotide states corresponding to the open state (M·ADP, M·ATPγS),[1] but an exception is the dinitrophenyl aminoethyl diphosphate BeFx complex (pdb 1D1A (19)). One possible explanation of the origin of the fluorescence enhancement associated with the open → closed transition is that the relay loop goes from a disordered to ordered state and internalizes the Trp-501 side chain during the ATPase cycle, so protecting it from solvent (H_2O) quenching. We have therefore carried out time-resolved fluorescence measurements on a mutant containing a single tryptophan residue at Trp-501 to test this idea.

Overall we find that the Trp-501 residue is static on the nanosecond time scale in all states (nucleotide and nucleotide-free) of the *Dictyostelium* motor domain. The anisotropy value is similar for all complexes and decays slowly with a time consistent with rotational motion of the whole motor domain (50–100 ns). However, the fluorescence intensity lifetime profiles and quantum yields suggest that in any one nucleotide state, the Trp-501 residue senses at least two or three different local environments on a time scale >5 ns to <20 μs. The fluorescence enhancement arises from a shift in the relative populations of these states that comprise both static and dynamically quenched components. Although accessibility to solvent water may contribute to quenching, interactions with nearby charged and polar groups are likely to be dominant factors. These results are compatible with the proposal that the relay loop remains structured throughout the ATPase cycle and maintains its contact with the converter domain (20) but that the environment of the tryptophan residue is affected by local rearrangements of the side chain and surrounding residues.

EXPERIMENTAL PROCEDURES

Materials—The cloning and preparation of a *D. discoideum* myosin II M761 motor domain containing a single tryptophan residue at position 501 was carried out as described previously (10) and is based on the expression vector developed by Manstein *et al.* (21). In this construct, denoted W501+, the nonresponsive tryptophan residues at positions 36, 432, and 584 were mutagenized to phenylalanine. A tryptophan-less construct, termed W−, was also made as a control in which all tryptophan residues were changed to phenylalanine. Nucleotides, NATA and human serum albumin (which contains a single buried tryptophan) were obtained from Sigma Chemical Co. (Poole, U. K.)

Steady-state Fluorescence Measurements—Steady-state fluorescence spectra and anisotropy were measured with an SLM 48000 spectrofluorometer (SLM Instruments, Urbana, IL) using a 5 mm path length cell (101.034-QS, Hellma, Westcliff-on-Sea, U. K.). For spectral measurements, tryptophan was excited with a Hg-Xe lamp at 297 nm with 1-nm slits to minimize photobleaching and to reduce inner filter effects arising from high nucleotide concentrations. Quantum yields were determined using the comparative method taking the value for tryptophan of 0.13 (22). Emission spectra were corrected using the calibration protocol supplied by SLM Instruments. Absorption spectra were measured using a Pye Unicam SP8–100 spectrophotometer.

Steady-state anisotropies were measured using the T format method with Glan-Thomson calcite prism polarizers. Tryptophan was excited at 295 nm with 2-nm slits, and the vertical (parallel) emission was detected through a monochromator set at 335 nm with 16-nm slits. The horizontal (perpendicular) emission was detected through WG320 and UG11 filters (Comar Instruments, Cambridge, U. K.). The anisotropy values (A) were calculated from the intensity values of the vertical and horizontal measurements with correction for the detector G value ($A = (I_v - G \cdot I_h)/(I_v + 2 \cdot G \cdot I_h)$). The G factor was calculated from the ratio of intensities (I_v/I_h) when the excitation light was horizontally polarized. The gain on the photomultipliers was adjusted so that the G factor was close to 1. However, we noted that the SLM automated polarization routine (48000 DOS version 2.1) gave erroneous values for the anisotropy because the background signal was not subtracted from intensities used to define the G value. Although this error may be negligible for strongly fluorescing samples, it was a significant factor in our measurements. For this reason we computed the anisotropy values independently from the measured intensity values. We also checked the anisotropy using the L format, so avoiding the use of the emission monochromator that makes a significant contribution to the G factor correction.

Transient fluorescence and absorption measurements were made using Applied Photophysics SX18MV stopped-flow apparatus with a xenon light source at 295 nm (2–4-nm slit width). Fluorescence emission was selected with WG320 and UG11 filters. All reactions were studied in a buffer comprising 40 mM NaCl, 20 mM TES, 1 mM $MgCl_2$ at pH 7.5 at 20 °C and the reagent concentrations stated refer to the reaction chamber.

Time-resolved Fluorescence Measurements—Time-resolved fluorescence measurements were carried out using the time-correlated single-photon counting method at the Rutherford Appleton Laboratory, Central Laser Facility. Samples (5–25 μM) were excited at 296 nm, achieved with a frequency-doubled, cavity-dumped, mode-locked synchronously pumped dye laser (Spectra-Physics model 3500) operating at 4 MHz with a pulse width of 10 ps. The fluorescence emission was collected via a WG335/UG11 filter combination (WG320 was used for tyrosine emission) using a MCP-PMT photomultiplier tube (Hamamatsu, R3809U) with response time of 85 ps. The WG335 filter was used in preference to the WG320 filter in these studies to minimize the potential scattering artifact and tyrosine contribution to the signal. Time-resolved anisotropy was measured through a film polarizer (Halbo Optics, DPUV-25) in the emission channel, and the vertical and horizontally polarized light was collected sequentially. The total emission intensity for lifetime measurements was calculated by summing $I_v + 2 \cdot I_h$. A wedge depolarizer was placed in front of the photomultiplier tube, and the G factor of the detector was confirmed as unity by excitation with horizontally polarized light. The data were collected in 1024 channels (width 40 ps) using the Becker and Hickl GmbH (Berlin) single time-correlated single photon counting pc card module (SPC-700). The standard functions of the single photon counting setup, such as time-to-amplitude converter and constant fraction discriminator, were computer-controlled with software supplied with the SPC-700 module.

RESULTS

Trp-501 Fluorescence Enhancement and Quantum Yield—The addition of ATP to the *D. discoideum* W501+ motor domain causes a large (30–90%) enhancement in tryptophan emission intensity (12). The percentage enhancement observed is critically dependent on the wavelength and band width of the excitation source and emission detector. Samples were excited at 295–297 nm to minimize the contribution from tyrosine fluorescence and inner filter effects on the addition of high adenine nucleotide concentrations. To obtain sufficient signal with xenon light sources, 2–4-nm slit widths were required, and particular care was required in analysis because of the extreme sensitivity to these extraneous contributions when operating at the edge of the excitation spectrum. The properties of the emission detector are also crucial because the enhancement in fluorescence is accompanied by about a 9-nm blue shift. For time-resolved measurements cut-off filters were used in the emission channel to maximize photon throughput, but this approach underestimates the percentage change in fluorescence compared with that determined from the integrated intensity of the complete corrected emission spectrum. On the

[1] The abbreviations used are: ATPγS, adenosine 5′-3-*O*-(thio)triphosphate; NATA, *N*-acetyl L-tryptophanamide; TES, *N*-tris(hydroxymethyl)methyl-2-aminoethanesulfonic acid; AMP·PNP, adenosine 5′-(β,γ-imino)triphosphate; mant-, 2′(3′)-*O*-(*N*-methylanthraniloyl); BeFx, beryllium fluoride with undetermined F content.

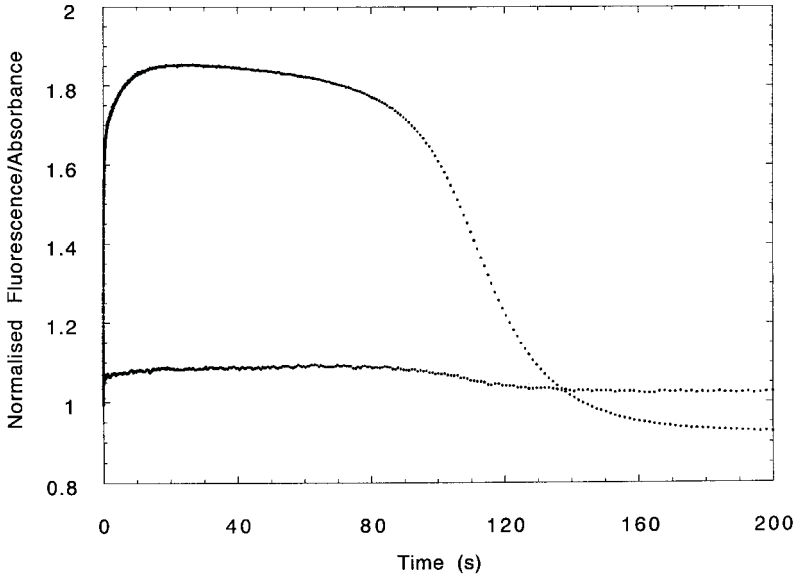

FIG. 1. **Enhancement in absorption and fluorescence of Trp-501 motor domain during the turnover of ATP.** 7.4 μM W501+ construct was mixed with 29 mM ATP in a stopped-flow device (reaction chamber concentrations), and the sample was illuminated with 295-nm light. The absorption and fluorescence (320-nm cut-off filter) were monitored in sequential pushes of the ram. The signals were normalized using a value of 0 for the buffer and 1 for the signal immediately after mixing (corresponding to the apo-state). The fluorescence change showed an 85% enhancement, and the absorbance increased by about 8% during the steady-state phase of the reaction.

other hand, spectral purity is more important for determining quantum yields, so these measurements were made on instruments with monochromators.

From the integrated emission intensities ATP gave an 85% enhancement in fluorescence, whereas ADP gave an 18% quench, in line with previous measurements on the W501+ construct (12). Early spectrophotometric studies on skeletal muscle myosin showed that there was a significant change in the absorption spectra induced by nucleotides (1). We reinvestigated this aspect with *D. discoideum* W501+ and found that at 297 nm there was a 13% increase in the absorption coefficient on ATP addition, but there was no detectable change with ADP at this wavelength. Thus, although there is a significant effect of ATP on the ground state properties of Trp-501, the fluorescence emission process is much more sensitive to the presence of nucleotide. This result is clearly demonstrated in a stopped-flow experiment using the same optics for the absorption and excitation process (Fig. 1). At wavelengths less than 290 nm the absorption change on ATP addition was inverted in sign. However, under these conditions the signal has a contribution from tyrosine residues, which outnumber the tryptophan residues by 29:1.

Quantum yields were calculated from the spectrally resolved emission data using free tryptophan as a standard (Table I). The addition of AlF_4^- to the W501+ construct in the presence of ADP generated a species whose fluorescence properties were very similar to the steady-state complex generated by the addition of ATP. The latter were measured over a period from 20 to 100 s when the fluorescence levels were almost constant. After the ATP was turned over (>200 s, depending on the [ATP]:[W501+] ratio), the fluorescence and absorption signals were similar to those generated by ADP addition alone. Addition of 50 μM sodium vanadate to the W501+ construct in the presence of ADP also caused a fluorescence enhancement, but the signal was reduced by 8% relative to that with the addition of AlF_4^- because of inner filter effects. We did not explore the vanadate complex further because the statically quenched component is difficult to evaluate in the presence of a high background absorbance.

Trp-501 Fluorescence Lifetime—Previous studies of the tryptophan fluorescence lifetime of myosin were carried out using a native protein fragment that contained 5 tryptophan residues and revealed 3 classes of tryptophans with lifetimes of 0.72, 4.5, and 8.8 ns (23). However, for most proteins it has been shown that a single tryptophan residue displays more than a single lifetime component and that site-directed mutagenesis is required for an unambiguous assignment of individual residues. In the case of the *D. discoideum* W501+ myosin motor domain we found that the lifetime decay was well fitted by two components with τ values of the order of 1 and 5 ns. Interestingly on addition of nucleotides, these lifetimes did not change significantly; rather, the fractional amplitudes changed (Fig. 2 and Table I). This agrees with the earlier studies (23) which showed that the major effect of ATP was to increase the fractional contribution of the 4.5-ns component. The change in mean lifetime is in the direction expected for the observed emission intensity *i.e.* ATP and ADP·AlF_4 cause a relative increase in the 5-ns component and an increase in the overall emission intensity, whereas ADP causes smaller changes in the opposite direction. Thus the nucleotide-induced changes in emission intensity contain a dynamically quenched component. However, quantitative comparison shows that the change in lifetime is only a partial explanation of the change in emission intensity. From the area under the normalized decay curves (Table I), ATP induces a 1.18 increase in mean lifetime relative to the nucleotide-free state, whereas ADP induces a reduction by 0.92. On the other hand, the measured emission intensity from the total counts (*i.e.* area under the un-normalized decay curves) was increased by 1.38 by ATP and reduced by 0.8 in the presence of ADP. The relative total photon counts are less than the maximum changes from the integrated fluorescence emission spectra (Table I) because light was collected from the red end of the spectrum (WG335 nm cut-off filter; see above). However, these values provide further evidence that the nucleotide-induced changes in Trp-501 fluorescence emission have both static and dynamic components. Thus, in a significant proportion ($\geq$ 60%; see below) of the population Trp-501 forms a ground state complex with a quenching center that changes the absorption characteristics and causes the excited state to return to the ground state by a nonradiative mechanism.

To estimate the contribution of the statically quenched component in the various nucleotide states, the quantum yields were compared with that of free tryptophan (0.13). If it assumed that free tryptophan in aqueous solution is quenched exclusively by a dynamic mechanism, then the intrinsic (natural) lifetime of tryptophan is about 16 ns. On this basis the fractional contributions of the static, 1-, and 5-ns components can be evaluated for each nucleotide state of the Trp-501 motor domain (Table II). This analysis reveals that the enhancement in Trp-501 fluorescence on addition of ATP is caused through a decrease in the statically quenched component and an increase in the 5-ns lifetime component with little change in the 1-ns

TABLE I
Trp-501 spectroscopic properties

State	Relative fluorescence emission[a]	Relative absorbance[b]	Quantum yield[c]	Relative quantum yield	Fluorescence lifetime					Anisotropy		
					A_1	τ_1	A_2	τ_2	Relative normalized area[d]	A_{ss}[e]	A_0[f]	ϕ
						ns		*ns*				*ns*
Apo	1.00	1.00	0.058	1.00	0.42	1.00	0.58	4.92	1.00	0.210	0.209	59 ± 4
ATP	1.85	1.13	0.095	1.64	0.25	1.11	0.75	4.78	1.18	0.216	0.191	59 ± 2
ADP	0.82	1.00	0.047	0.82	0.45	0.91	0.55	4.74	0.92	0.214	0.194	54 ± 2
ADP · AlF	1.88	1.14	0.095	1.64	0.27	1.37	0.73	4.82	1.19	0.216	0.203	68 ± 4[g]

[a] From integration of the corrected fluorescence emission spectra with excitation at 297 nm with a xenon-mercury lamp. Note that the observed enhancement of Trp-501 on ATP addition is instrument-dependent and is typically 1.4–1.8 depending on the wavelength and band width of the emission filter or monochromator (12) as well as the excitation source.
[b] Relative absorbances were measured at 297-nm and 1-nm band width. Smaller changes are observed in the stopped-flow apparatus because of the larger slit width (>2 nm).
[c] Calculated relative to free tryptophan quantum yield (0.13).
[d] Relative normalized areas were calculated from the lifetime decays in which $A_1 + A_2 = 1$. The total count, selected with a 335-nm cut-off filter, indicated that the ATP enhanced the fluorescence by 1.38.
[e] Steady-state anisotropy measured on SLM fluorometer with prism polarizers.
[f] Anisotropy of slow phase extrapolated to zero.
[g] ADP · AlF_4^- data collected in different run where rigor $\phi = 64 \pm 4$ ns. Apart from the time-resolved anisotropy data, standard errors in the fitted parameters were <2% of the value given. Parameters deduced from different experimental runs (n = 2–7) agreed within 10% of the values given.

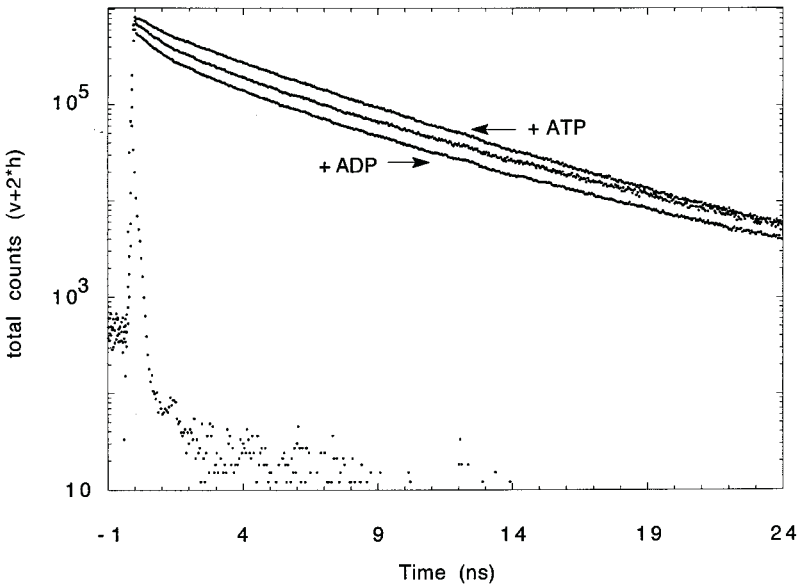

FIG. 2. **Fluorescence intensity decay of 5.3 μM W501+ motor domain in the absence and presence of 1 mM ATP or 0.6 mM ADP.** Photon counts were pooled from data sets obtained using a horizontal and vertical polarizer in the emission channel to give the total photon count (v + 2 h). The *solid points* are the lamp pulse profile as determined using a scattering solution in the sample position. The *middle* decay curve was obtained in the absence of nucleotide. Note that the addition of ATP caused a net enhancement and ADP a net quench in photon emission. The decay profiles remain almost parallel because of the dominant 5-ns decay component present in all samples. Fitting the decays to a two-exponential function revealed the lifetimes and amplitudes given in Table I.

lifetime component. The subsequent net quench observed after turnover to ADP arises from an opposite shift in the fractions of statically quenched and 5-ns components, again with little change in the 1-ns component.

As a control sample, we measured the fluorescence lifetime of human serum albumin under the same conditions and found two components with $\tau_1 = 1.3$ ns ($a_1 = 0.32$) and $\tau_2 = 6.0$ ns ($a_2 = 0.68$), in fair agreement with values of $\tau_1 = 1.42$ ns ($a_1 = 0.16$) and $\tau_2 = 6.06$ ns ($a_2 = 0.84$) determined by phase fluorometry (24). We also measured the lifetime of NATA and found a two-component fit with $\tau_1 = 0.98$ ns ($a_1 = 0.24$) and $\tau_2 = 4.7$ ns ($a_2 = 0.76$). Other workers have reported satisfactory fits to a single component with lifetime of 3.2 ns (22). Lifetime components of 5-ns in tryptophan analogs have been ascribed to photoconversion of the indole ring during the exposure to the excitation light. This does not appear to be a contributory factor in our measurements of the *D. discoideum* W501+ myosin motor domain, at least. When the ATP was hydrolyzed after several hours of incubation, the emission intensity fell, and the lifetime distribution returned to that characteristic of the ADP state (*i.e.* a decrease in the 5-ns component).

As a control for the contribution of tyrosine fluorescence to the signal, a tryptophan-less construct, W−, was investigated using the same instrumental settings. When fluorescence was detected through a 335-nm cut-off filter very little signal was obtained (see Ref. 12). With a 320-nm cut-off filter sufficient counts were obtained to reveal lifetimes of 0.4 ns ($a_1 = 0.72$) and 3.4 ns ($a_2 = 0.28$). These data indicate that there is negligible tyrosine contribution to the lifetimes resolved in the W501+ construct at wavelengths >335 nm, despite the presence of 29 tyrosine residues.

TABLE II
Proportion of static and dynamically quenched species based on lifetime data and quantum yields relative to free tryptophan

The ratio of 1- and 5-ns components is defined by the observed intensity decay curves. The fraction of static quenched component (*i.e.* the fraction that loses energy via a nonradiative pathway) is assigned to account for the observed quantum yield relative to free tryptophan, assuming the later has a natural lifetime of 16 ns.

Nucleotide state	Static component	1-ns component	5-ns component
Apo	0.71	0.12	0.17
ATP	0.60	0.10	0.30
ADP	0.76	0.11	0.13
ADP · AlF_4	0.60	0.10	0.30

Trp-501 Steady-state and Time-resolved Anisotropy—Steady-state fluorescence anisotropy measurements showed

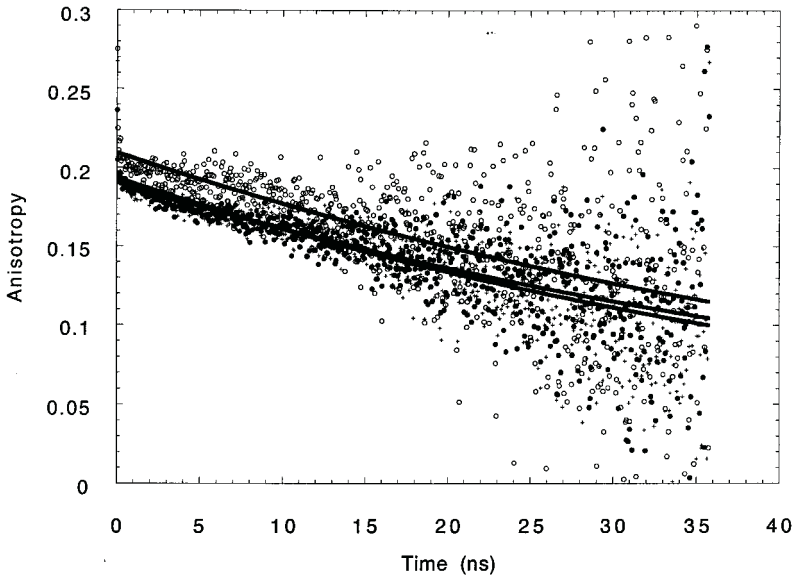

FIG. 3. **Time-resolved anisotropy curves for 5.3 μM W501+ motor domain in the absence (○) and presence of 1 mM ATP (●) or 0.6 mM ADP (+) at 20 °C.** The *solid line* shows a single exponential fit to the data to give rotational correlation times shown in Table I. The slightly higher limiting anisotropy value in the absence of nucleotide was not a reproducible feature.

that there was no significant change in anisotropy of tryptophan in the *D. discoideum* W501+ construct on addition of ATP or ADP (Table I). The values observed of 0.21 at 20 °C were close to the limiting value of 0.23 measured in the presence of 90% glycerol at 9 °C. In contrast, when the *D. discoideum* W501+ motor domain was denatured with 6.6 M guanidinium hydrochloride, the anisotropy fell to 0.1. These data suggest that the tryptophan is relatively immobile in all native states of W501+, and reducing the rotational rate of the protein by increased viscosity has only a limited effect. The difference between the limiting anisotropy value and the theoretical maximum value of 0.4 is indicative of a difference in the angle between the absorption and emission dipoles and/or small amplitude, high frequency motions ($t \ll 1$ ns) that lead to partial depolarization. The value of 0.23 is close to that observed for immobilized tryptophan in model studies, but this measurement shows a very steep dependence of excitation wavelength in the region of 290–300-nm excitation (22).

These steady-state studies were complemented with time-resolved anisotropy measurements. As expected, a high limiting anisotropy value was observed (around 0.2) with only a slight decay over 40 ns in all records (Fig. 3). The slightly lower limiting anisotropy (A_o) compared with the steady-state measurements (A_{ss}) could be a result of the lower discrimination of the film polarizers compared with the Glan-Thomson prisms. The first time point, coincident with the peak of the laser pulse, showed a slightly higher anisotropy value (0.24–0.27), but the values after 80 ps were not significantly different from that of the major decay profile. The first two time points may indicate a very rapid but limited amplitude motion of Trp-501; however, any breakthrough scattered light would also contribute to this signal, and we have not attempted to analyze it further. We focus on the major slow phase in the anisotropy decay.

The short lifetime of tryptophan results in a limited ability to follow the anisotropy decay beyond 10–20 ns. However, because a protein solution is randomly oriented, there should be no residual anisotropy at infinite time, and the data may be analyzed by force fitting it to an exponential function that decays to zero. With such an analysis, single rotational correlation times, ϕ, of the order of 50–70 ns, were obtained for all nucleotide states of the *D. discoideum* motor domain (Table I). We found no systematic difference in ϕ for the different nucleotide states in three independent runs. This time scale is close to that expected for the whole protein molecule. Although we cannot rule out that there is a second slower rotational correlation time, the calculated limit from the whole protein motion indicates that this would not be longer than about 150 ns. Whole molecule relaxation times from electric birefringence of about 250 ns have been reported for a myosin subfragment containing the complete regulatory domain (25) which, when extended, is nearly 80% longer than the *D. discoideum* domain motor domain used here. As a control sample we measured the anisotropy decay of human serum albumin (molecular weight 66,000) under the same conditions and found the rotational correlation time, ϕ, of the slow component to be 39.5 ns at 20 °C, in good agreement with 38.6 ns determined by phase fluorometry (24). Overall, the time-resolved anisotropy data corroborate the steady-state values and demonstrate that the Trp-501 has little independent motion relative to the rotational correlation time of the whole protein in all nucleotide states examined.

DISCUSSION

The photophysics of tryptophan in proteins is a complex topic, but several key features have been elucidated over the last few decades through the use of model compounds and single tryptophan-containing proteins (22, 26). The indole ring has two emission dipoles La and Lb that are oriented at 90° to each other. The former is almost parallel to the absorption dipole and is responsible for high positive anisotropy values when immobilized. At an excitation wavelength of 295 nm and emission collection >330 nm, the Lb emission is unlikely to make any significant contribution to the observed signal (22). However, tryptophan emission remains complex because different rotamers bring the indole ring into proximity with different groups whose quenching efficiency varies. In free tryptophan, the interconversion of rotamers is slower than the fluorescence emission process, leading to a non-single exponential profile. Under aqueous conditions at pH 7, two phases are resolved (with τ around 0.5 and 3.1 ns) with the shorter lifetime attributed to quenching by the positively charged amino group that is in closest proximity in one rotamer (27). This short lifetime component is lacking in the NATA derivative. Tryptophan residues within proteins are less susceptible to quenching from their own uncharged α-amide and α-carbonyl groups, but they may have additional interactions with side chains brought into close proximity within the tertiary structure. From the quantum yield of around 0.13 for free tryptophan and lifetimes of 0.5 and 3.1 ns in aqueous solvents, the intrinsic lifetime of tryptophan is calculated to be about 16 ns, assuming that the quenching mechanism is exclusively dynamic in nature. For

tryptophan residues in proteins, lifetimes typically range from 0.1 to 10 ns (28), demonstrating that even when protected from solvent, interactions with other side chains or chromophores provide an efficient route for relaxation from the excited state. Groups that have been suggested to contribute to quenching within proteins are the side chains of lysine, tyrosine, glutamine, asparagine, glutamic acid, aspartic acid, cysteine, and histidine (26) as well as the backbone carbonyl groups (29). In general, multiphasic or stretched exponential kinetics are to be expected for the lifetimes of single tryptophan residues in proteins, and this is born out in practice. Single exponential kinetics are only observed if the local environment is homogeneous or nearby groups are in very rapid motion (subnanosecond) to average out any inhomogeneity. Even in protein crystals where a tryptophan residue is clearly resolved and appears to reside in a unique orientation, fluorescence lifetime measurements of the crystalline state show multiple phases (27). These results are not incompatible because the existence of multiple orientations may go undetected in fitting the electron density. Resolutions in excess of 1.5 Å are generally required to resolve multiple orientations of side chains in protein crystals.

With this background, it is not surprising that the fluorescence lifetime of Trp-501 in the *D. discoideum* myosin motor domain deviates from single exponential kinetics. More unexpected is the finding that changes induced by nucleotide appear to be associated with a relative change in the amplitudes of the lifetime components with little change in the associated time constants, which remain at about 1 and 5 ns. This finding is to some extent linked to fitting the data to a biexponential function. When fitted to a triexponential function there was no improvement in fit for the data obtained in the presence of ATP and ADP·AlF_4^- and only a marginal improvement for the data obtained in the absence of nucleotide and ADP (with lifetimes 0.7, 3, and 7 ns). This is a reflection of the ill conditioned nature of exponential functions. Nevertheless the data do indicate a rather limited contribution from any species with a lifetime between 1.5 and 3 ns or greater than 7 ns, independent of the fitting procedure. For the purpose of discussions we will consider that the lifetime distributions to fall into two classes with values distributed around 1 and 5 ns. On the basis of an intrinsic (natural) lifetime of tryptophan of about 16 ns, the data obtained with Trp-501 can be analyzed in terms of fractions of statically and dynamically quenched components to account for the overall quantum yield of different nucleotide states (Table II). The analysis indicates that the major effect of nucleotide is to shift the relative proportions of static and 5-ns lifetime components, with little effect on the 1-ns component. This characteristic has been seen in some other native proteins where it has been interpreted as evidence for microstate reshuffling (30). Microstates refer to conformations of the protein that are in rapid equilibrium compared with gross conformational transitions induced by ligand binding (Fig. 4). Microstates must have lifetimes >5 ns so that specific components are resolved in the lifetime analysis. However, temperature jump studies on W501+ motor domain indicate that the fluorescence quenching processes re-equilibrate with a time constant of <20 μs.[2]

One possible interpretation of the data is that Trp-501 is located in a partially solvent exposed, dynamic region of the protein such that the side chain interacts with solvent water and other nearby side chains on the nanosecond time scale to effect collisional quenching. Changes in gross protein conformation associated with different nucleotide states cause a change in the weighting of the various interactions experienced by Trp-501 but not of their nature. The large and nucleotide-independent anisotropy value (~0.2) of Trp-501 and the long rotational correlation time (~60 ns) argue that the Trp-501 side chain itself is relatively static, and hence the residues with which it interacts may provide the dynamics associated with the fluorescence relaxation process (1–5 ns). The microstates may correspond to different rotamers of the Trp-501 side chain which interconvert on a time scale of >60 ns to expose the indole ring to different environments (Fig. 4). It appears unlikely that the relay loop is melted in the open state, otherwise the anisotropy values would be expected to be close to that of the denatured state ($A = 0.1$). However, because the anisotropy decay appears limited by the rotation of the whole domain, it is possible that Trp-501 shows different rotational dynamics in different biochemical states but on a time scale of >60 ns. The failure to resolve the relay loop in many crystal structures therefore appears to arise from static disorder. This conclusion is in accord with cross-linking studies (20) that show that the relay loop bearing Trp-501 remains in close contact with the converter domain throughout the actin-activated ATPase cycle (between residues Ile-499 and Arg-738 at least).

Another complication that must be considered is that although x-ray crystallography of myosin may yield a particular structure for a particular bound nucleotide, kinetic studies show that a number of states are often significantly occupied in solution. In particular, the myosin-ADP·BeFx and AMP·PNP complexes show multiple states whose equilibrium distribution is particularly temperature-sensitive over the 0–20 °C range (12). We have therefore focused on other complexes (ADP and ADP·AlF_4^-) in our lifetime characterization study. Nevertheless, there is likely to be some degree of heterogeneity in all nucleotide states in solution. For example, during the steady-state hydrolysis of ATP by the *D. discoideum* motor domain, there are detectable levels of the M†·ATP, M*·ADP·P_i, and M†·ADP states (Reaction 1) with occupancies of ~29, 70, and 1% at 20 °C (12). It is therefore pertinent to question whether the M*·ADP·P_i state itself could be associated with a single 5-ns lifetime component and whether the observed heterogeneity (Table I) arises from the other nucleotide states rather than microstates within a single nucleotide state. Relevant to this argument is the possibility that the 5-ns component is underestimated in the presence of ATP after selection by the WG335 cut-off filter because the spectrum is blue shifted. Correction on the basis of the observed enhancement (1.38) compared with the integrated corrected emission spectra (1.85, Table I) suggest that the corrected ratio in the presence of ATP may be $a_1 = 0.2$ for the 1-ns component and $a_2 = 0.8$ for the 5-ns component. Given the uncertainties in the exact distributions, it is possible that the M*·ADP·P_i state could be associated with essentially a single 5-ns lifetime state, and the 1ns component arises from the M†·ATP and M†·ADP states. However, there is still a requirement for a statically quenched microstate of M*·ADP·P_i to account for the relatively low quantum yield observed in the presence of ATP compared with that of free tryptophan and NATA. Therefore M*·ADP·P_i comprises at least two microstates. In the presence of saturating ADP, >95% of the myosin should be in the M†·ADP state, yet at least three spectroscopic microstates are present (statically quenched, 1-ns and 5-ns components). Likewise, there are at least three microstates for the nucleotide-free myosin (Table II). It should be noted that the microstates within each class are not necessarily identical in local conformation, and different quenching groups might be involved in different biochemical states. Indeed, the quench in fluorescence emission intensity observed in the M†·ADP is accompanied by a blue shift, as is the enhancement observed in M*·ADP·P_i, implying the

[2] A. Málnási-Csizmadia and C. R. Bagshaw, unpublished observations.

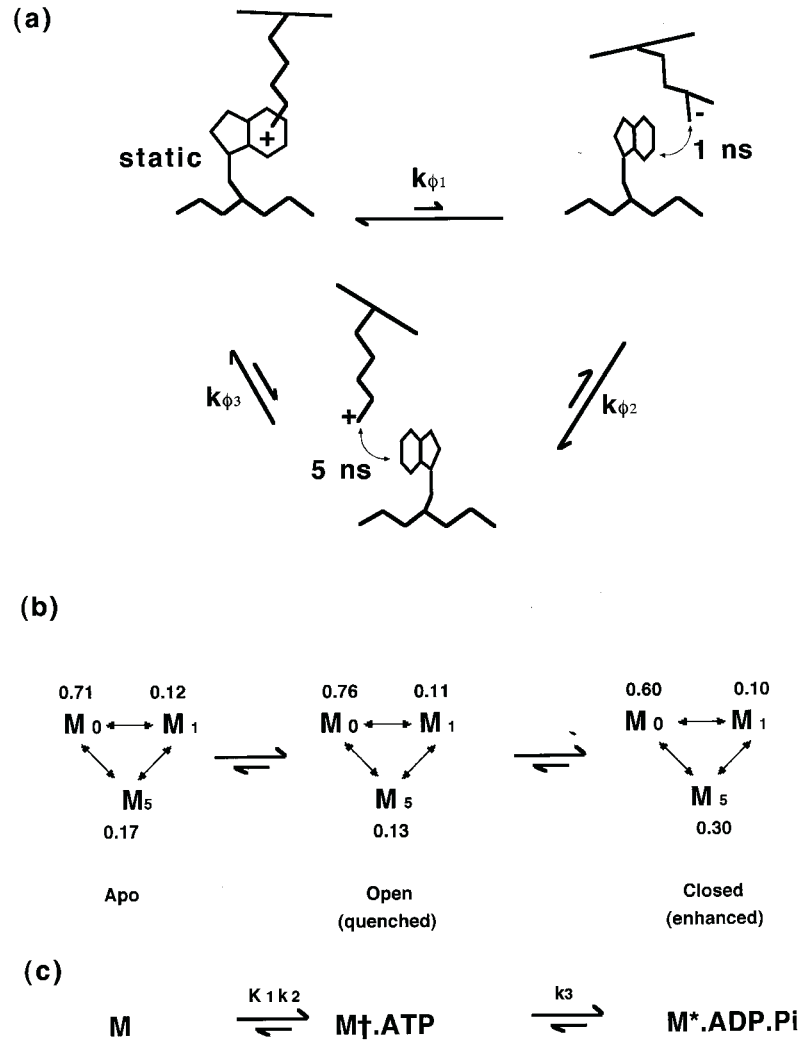

FIG. 4. **Schematic diagram to show the interconversion of Trp-501 microstates and their relationship to nucleotide states.** *Panel a*, the mechanism of Trp-501 fluorescence quenching involves three microstates, one of which (M_0) is statically quenched (effective fluorescence lifetime = 0), whereas the other two (M_1 and M_5) have lifetimes of close to 1 or 5 ns. Lifetimes are reduced over the natural lifetime of tryptophan by collisional processes that may involve dynamic interactions with charged or polar side chains, backbone carbonyl groups, or solvent water. The interactions shown are chosen arbitrarily for illustration, but potential candidates can be identified (see "Discussion"). Interconversion between microstates must be slower than 5 ns and could involve different rotamers of Trp-501 as illustrated. This would be in accord with the long rotational correlation times reported in Table I, *i.e.* $k\phi$ values $< 20\ \mu s^{-1}$. *Panel b*, microstates are in rapid equilibrium compared with chemical steps and gross conformational changes (*i.e.* $k\phi$ values $>50\ ms^{-1}$ from temperature jump measurements) and are distributed according to the fractional occupancy shown in Table II. Accordingly a unique pathway of interconversion between microstates cannot be defined during transitions between chemical or gross conformational states because they remain close to equilibrium throughout. Note that the decrease in the 5-ns component largely accounts for the observed percentage quench in Trp-501 emission intensity on binding ADP (to give the open state), whereas the increase in the 5-ns component accounts for the percentage enhancement on forming the closed state (hydrolysis to $M^*{\cdot}ADP{\cdot}P_i$). *Panel c*, corresponding transitions as applied to the first three chemical steps of the ATPase pathway. Rate constants estimated by transient kinetic methods are macroscopic rate constants for the overall population of microstates. It is assumed in the scheme shown that ATP quenches to the same degree as ADP; this has not been proven (12). From stopped-flow measurements it is likely k_2 is $>200\ s^{-1}$, and $k_3 = 30\ s^{-1}$ (12). However, perturbation methods indicate that the open → closed transition may occur as fast at $1{,}000\ s^{-1}$ but requires hydrolysis to drive the equilibrium toward the closed state (A. Málnási-Csizmadia and C. R. Bagshaw, unpublished observations).

intermediate intensity of the apo-state is not simply a mixture of the these two (12).

Interestingly, the fluorescence enhancement and quantum yield observed in the presence of $ADP{\cdot}AlF_4$ is very similar to that seen in the presence of ATP. Given that the steady-state ATPase complex contains a small but significant fraction of quenched nucleotide states (M†·ATP and M†·ADP), it might be expected that $M^*{\cdot}ADP{\cdot}AlF_4$ would show up to a 30% higher fluorescence emission than in the presence of ATP. These data suggest that $M^*{\cdot}ADP{\cdot}AlF_4$ could be in equilibrium with a small amount of $M\dagger{\cdot}ADP{\cdot}AlF_4$ state at 20 °C. Temperature and pressure jump experiments are in progress to investigate the kinetics of reequilibration between different bound-nucleotide states that are not resolved by rapid mixing methods.

The ATP-induced enhancement of the relay loop tryptophan (Trp-501 or equivalent residue) appears to be a conserved property of myosin II molecules. It is difficult to compare the magnitude of enhancement in different species in the literature because the observed values are instrument-dependent, but the direction of the change is common. On the other hand, although ADP generally induces a smaller change in fluorescence emission, its effect appears to be species-specific. A quench is observed with *D. discoideum* myosin (12), but an enhancement is observed with a smooth muscle myosin construct (10). This difference could reflect either a different gross conformation (*i.e.* ADP is able to partially induce the closed conformation in smooth myosin) or a difference in the local amino acid structure around the relay loop tryptophan. Comparisons of the x-ray

structures (5, 6) reveal several side chains and backbone carbonyl groups that could contribute to quenching, and these are generally highly conserved residues. Candidates within the vicinity (<1 nm) of the Trp-501 side chain are Glu-490, **Gln-491**, Glu-493, **Tyr-494**, Ile-199 (backbone carbonyl), Asn-500, Trp-501 (backbone carbonyl), **Thr-502** (backbone carbonyl), Phe-501 (backbone carbonyl), Lys-690 (including backbone **carbonyl**), and Gly-691 (backbone carbonyl). Residues in bold are within 0.5 nm of Trp-501 in the closed-state (M·ADP·Vi) and are the prime candidates for involvement in quenching. Unfortunately, there are no structures of the *D. discoideum* motor domain with sufficient resolution in the relay loop to define the position of the corresponding residues in the open state (19). Nevertheless, this region can be compared with motor domains from other species. However, from the limited comparison possible to date, there is no residue that can be uniquely identified with the dequenching process observed in the presence of ATP.

The finding that the Trp-501 is effectively immobile on the time scale of fluorescence emission has bearing on fluorescence energy transfer measurements. For example, Yengo *et al.* (10) assumed free rotation or random orientation of the equivalent Trp-512 residue in smooth myosin in calculating the distance from mant-nucleotide bound at the active site. Previous anisotropy studies on mant-nucleotide complexes showed that the acceptor mant group is relatively static when bound to myosin (31, 32). Thus, such distance calculations using the Forster equation will be extremely dependent on the relative orientation of the tryptophan donor and mant-acceptor dipoles. Angles in the range of about 35° from the optimal dipole orientation could account for the underestimate of the separation by fluorescence resonance energy transfer of 26 Å (10) compared with 45–50 Å measured from the crystal structure of the M·mant·ADP·BeFx complex. It should be noted that Trp-501 was not resolved in this structure, but the adjacent residue Asn-500 was assigned and therefore limits the position of Trp-501 (32). It is likely that the apparent 8 Å movement of the Trp-512 residue in different nucleotide states (10) is a reflection of different orientations of the tryptophan (as might occur with different rotamer distributions) rather than translational movement. Alternatively, the fluorescence resonance energy transfer measurements (10) may have a differential contribution from the numerous tyrosine residues, particularly as 285-nm excitation was used. In principle, changes in the predominant tryptophan side chain orientation should be revealed in the time-resolved fluorescence anisotropy studies because the motor domain is not spherical, and therefore different probe orientations should have different limiting rotational correlation times. However, the dimensions of the motor domain of $\sim 100 \times 60 \times 40$ Å would not result in a strong dependence, particularly if the tryptophan reoriented around the shorter axes. Notably, we found that the rotational correlation time of a single tryptophan *D. discoideum* motor domain mutant, F129W, measured under the same conditions was around 100–120 ns compared with 60 ns for Trp-501. This suggests that the emission dipole of the former is aligned predominantly along the long axis of the motor domain and/or that Trp-501 has a small degree of independent motion.

In conclusion, the time-resolved fluorescence data presented here show that Trp-501 experiences at least three different microenvironments. The coupling between the occupancy of the nucleotide site and the Trp-501 environment does not correspond to a simple one-to-one relationship. Rather, nucleotide binding allows the Trp-501 side chain to redistribute among different environments on a time scale of >5 ns and <20 μs. It is therefore not possible to equate a particular nucleotide state or a particular gross conformation (open or closed state), to a unique set of coordinates for Trp-501 and its surrounding residues, as might be implied by some crystal structures. This behavior has been reported in other probe studies that reflect gross conformational rearrangements of the myosin motor domain (33, 34). Nevertheless, the crystal structures are valuable in defining the potential environments that surround the Trp-501 side chain. We find no evidence that the relay loop is dynamically disordered on the nanosecond time scale in the open conformation, as might be surmised from the crystal data. In this respect our data are concordant with that of Shih and Spudich (20) showing that the relay loop does not make any large scale rearrangements relative to the converter region during ATPase activity.

Acknowledgments—We thank William Shih and Jim Spudich for an advanced copy of their manuscript and discussions. We thank Tony Parker for access to the Central Laser Facility.

Note Added in Proof—A crystal structure (Protein Data Bank accession code 1G8X) of an engineered *D. discoideum* myosin motor domain locked in the open state has recently been published in which the two molecules in the unit cell have the same gross conformation, but different rotamers of Trp-501 are resolved (Kliche, W., Fujita-Becker, S., Kollmar, M., Manstein, D. J., and Kull, F. J. (2001) *EMBO J.* **20,** 40–46). This structure also identifies the side chain of Arg-747 as a potential quenching group in the open state.

REFERENCES

1. Morita, F., and Yagi, K. (1966) *Biochem. Biophys. Res. Commun.* **22,** 297–302
2. Bagshaw, C. R., Eccleston, J. F., Trentham, D. R., Yates, D. W., and Goody, R. S. (1972) *Cold Spring Harbor Symp. Quant. Biol.* **37,** 127–135
3. Werber, M. M., Szent-Györgyi, A. G., and Fasman, G. D. (1972) *Biochemistry* **11,** 2872–2883
4. Rayment, I., Rypniewski, W. R., Schmidt-Bäse, K., Smith, R., Tomchick, D. R., Benning, M. M., Winkelmann, D. A., Wesenberg, G., and Holden, H. M. (1993) *Science* **261,** 50–58
5. Fisher, A. J., Smith, C. A., Thoden, J., Smith, R., Sutoh, K., Holden, H. M., and Rayment, I. (1995) *Biochemistry* **34,** 8960–8972
6. Smith, C. A., and Rayment, I. (1996) *Biochemistry* **35,** 5404–5417
7. Dominguez, R., Freyzon, Y., Trybus, K. M., and Cohen, C. (1998) *Cell* **94,** 559–571
8. Houdusse, A., Kalabokis, V. N., Himmel, D., Szent-Györgyi, A. G., and Cohen, C. (1999) *Cell* **97,** 459–470
9. Batra, R., and Manstein, D. J. (1999) *Biol. Chem. Hoppe-Seyler* **380,** 1017–1023
10. Yengo, C. M., Chrin, L. R., Rovner, A. S., and Berger, C. L. (2000) *J. Biol. Chem.* **275,** 25481–25487
11. Onishi H, Konishi, K., Fujiwara, K., Hayakawa, K., Tanokura, M., Martinez, H. M., and Morales, M. F. (2000) *Proc. Natl. Acad. Sci. U. S. A.* **97,** 11203–11208
12. Málnási-Csizmadia, A., Woolley, R. J., and Bagshaw, C. R. (2000) *Biochemistry* **39,** 16135–16146
13. Hiratsuka, T. (1992) *J. Biol. Chem.* **267,** 14949–14954
14. Park, S., Ajtai, K., and Burghardt, T. P. (1997) *Biochemistry* **36,** 3368–3372
15. Park, S., and Burghardt, T. P. (2000) *Biochemistry* **39,** 11732–11741
16. Geeves, M. A., and Holmes, K. C. (1999) *Annu. Rev. Biochem.* **68,** 687–728
17. Bagshaw, C. R., Eccleston, J. F., Eckstein, F., Goody, R. S., Gutfreund, H., and Trentham, D. R. (1974) *Biochem. J.* **141,** 351–364
18. Johnson, K. A., and Taylor, E. W. (1978) *Biochemistry* **17,** 3432–3442
19. Gulick, A. M., Bauer, C. B., Thoden, J. B., Pate, E., Yount, R. G., and Rayment, I. (2000) *J. Biol. Chem.* **275,** 398–408
20. Shih, W. M., and Spudich, J. A. (2001) *J. Biol. Chem.* **276,** 19491–19494
21. Manstein, D. J., Schuster, H.-P., Morandini, P., and Hunt, D. M. (1995) *Gene* (*Amst.*) **162,** 129–134
22. Lakowicz, J. R. (1999) *Principles of Fluorescence Spectroscopy*, 2nd Ed. Kluwer Academic Publishers, Norvell, MA
23. Torgerson, P. M. (1984) *Biochemistry* **23,** 3002–3007
24. Lakowicz, J. R., and Gryczynski, I. (1992) *Biophys. Chem.* **45,** 1–6
25. Highsmith, S., Polosukhina, K., and Eden, D. (2000) *Biochemistry* **39,** 12330–12335
26. Chen, Y., and Barkley, M. D. (1998) *Biochemistry* **37,** 9976–9982
27. Dahms, T. E. S., and Szabo, A. G. (1997) *Methods Enzymol.* **278,** 202–221
28. Beecham, J. M., and Brand, L. (1985) *Annu. Rev. Biochem.* **54,** 43–71
29. Sillen, A., Fernando-Díaz, J., and Engelborghs, Y. (2000) *Protein Sci.* **9,** 158–169
30. Gastmans, M., Volckaert, G., and Engelborghs, Y. (1999) *Proteins Struct. Funct. Genet.* **35,** 464–474
31. Rosenfeld, S. S., Xing, J., Rener, B., Lebowitz, J., Kar, S., and Cheung, H. C. (1994) *J. Biol. Chem.* **269,** 30187–30194
32. Bauer, C. B., Kuhlman, P. A., Bagshaw C. R., and Rayment, I. (1997) *J. Mol. Biol.* **274,** 394–407
33. Baker, J. E., Brust-Mascher, I., Ramachandran, S., LaConte, L. E. W., and Thomas, D. D. (1998) *Proc. Natl. Acad. Sci. U. S. A.* **95,** 2944–2949
34. Shih, W. M., Gryczynski, Z., Lakowicz, J. R., and Spudich, J. A. (2000) *Cell* **102,** 683–694